

Research Article

Welding Fume Reduction in Flux Cored Wire Arc Welding using Nanoparticles-Shielding Gas Mixture

Isaratat Phung-on^{1*}

Received: 1 January 2022

Revised: 31 March 2022

Accepted: 23 April 2022

ABSTRACT

Welding fume could be harmful to welders and operators, especially to the respiratory system. In general, welding fumes could form in various types of oxides such as Fe_3O_4 or MnFe_2O_4 . There have been various methods for both extracting and reducing fume formation but with some limitations. This research introduced a novel development by using a mixture of ZnO nanoparticles mixed into the shielding gas stream in the flux-cored wire arc welding process. By utilizing the photocatalytic reaction producing free electrons to neutralize the oxide metal, the fume formation would be suppressed. The system was designed as add-on equipment compiling with the existing operating parameters. Nanoparticle could reduce fume generation rate from 0.84 to 0.58 g/min (30.28%) and 0.66 to 0.46 g/min (29.65%) at shielding gas flow rate of 25 and 15 L/min, consecutively. Its robustness was applicable for %fume generation rate reduction at 29.95% and 21.33%, at welding current of 200 A and 120 A. The weld performance test conformed to the requirements of ASME BPVC.IX. Microstructure and chemical composition showed no evidence of crack and nanoparticle residue. This fume reduction utilizing nanoparticles is effective without a detrimental effect on weld performance. There is only a little adjustment during installation. Owing to its design as a refillable canister, it is convenient for the same usable duration as 1 cylinder of CO_2 gas.

Keywords: Welding Fume; Fume Reduction; Nanoparticles

¹Maintenance Technology Center, ISTRS, King Mongkut's University of Technology Thonburi, Bangkok, Thailand

*Corresponding author, email: isaratat.phu@kmutt.ac.th

Introduction

Welding fume is a persisting problem in both manufacturing and fabrication. There are many health problems affecting welders and related operators, especially for the respiratory system, cancer, or neuro-system [1]. Welders with a smoking habit could have more risk for pulmonary illness [2]. In comparison to other types of work, welding could pose more cancer risks [3]. That evidence has drawn attention to occupational health and safety in welding as well as environmental, social life cycle [4].

Welding fume was characterized by presenting alkali fluoride constituent phases together with Fe-Mn oxides [5]. This was confirmed by the results of the study of an Electrical Low-Pressure Impactor (ELPI) for collecting several sizes of welding fume and evaluating their compositions [6]. Another study showed the differences in fume generation rate among the types of welding electrodes: cellulose, rutile, and basic [7]. The size of fumes collected was very small below 2.5 microns in the majority. Due to their small size, the fume could spread over a long distance up to 200 centimeters from the welding location [8]. Even in the open area such as at the shipyard, welding fume is also a problem. According to the study, the respirable Manganese (Mn) was over the safety limit [9]. However, it could be reduced by using the Local Exhaust Ventilation (LEV) [10], but it was not convenient for the welders.

In some cases, such as for high Mn consumables, the constituents might have Mn substitution to Fe forming the $MnFe_2O_4$ or $FeMn_2O_4$ showing its contribution to the fume formation [11]. From the fume constituent aspect, fume generation models have been developed showing the contribution of Fe and Mn. A model has been developed [12] in conjunction with theoretical and empirical information. Both Fe and Mn concentrations could be estimated. Welding process parameters also have contributions to fume formation. Dennis et al. [13] showed the effects of welding current, wire feed speed, and wire compositions on the fume formation model in the gas metal arc welding process.

Many methods have been developed to mitigate fume formation and its effects. Fume extractors would be the easiest method to take the fume out from the operating area. A lightweight LEV has been developed with a weight of only 50 kilograms for easy carrying to the welding area [14]. However, in some cases, it was not convenient and limited to the applicable locations. A handheld extractor was also designed to be attached to the welding gun [15] for more convenience and effectiveness. Still, it might compromise the loss of shielding gas from too strong suction of the fume extractor. Another concept was by utilization of arc stability and welding parameters such as the pulse-arc studied [16, 17]. The limitation of this concept was the cost of welding power supply and knowledge of the welders on the arc physic.

The composition of weld consumables was another concept to control both types and concentrations of the welding fume. Changing alloy contents either metal core-wire or flux covered could be helpful for arc stability and species forming the fume, especially for Hexavalent Chromium (Cr^{6+}) formation. Cr^{6+} is a lung carcinogen with some required limited exposure. Cr-free weld consumables were successfully developed aiming to reduce the Cr^{6+} formation [18]. However, altering the alloy contents might affect the properties and performances of the weldment requiring more tests and approvals. As an alternative, nanoparticles could be implemented on the welding electrodes for fume

reduction. TiO₂ nanoparticles could be applied to the metal core wire of welding electrodes [19]. This could help with arc stability and reduce fume generation.

This study introduced a novel development of using only the tiny amount of nanoparticles mixing into the stream of shielding gas in the flux-cored wire welding (FCAW) process without adjustment to the existing welding process parameters. The system has been designed as an add-on accessory consisting of a base unit and a refillable canister containing the nanoparticle mix. Fume generation rate was measured for its usability ranges at various welding current levels. The amount of nanoparticles spending rate was also measured to determine the period before refilling the canister. Weld performance tests were implemented to determine any detrimental effects that might occur. Microstructures and Scanning Electron Microscope with Energy Dispersive Spectrometry (SEM/EDS) were also utilized to determine residues of nanoparticle contents in the weld metal.

Materials and Methods

Nanoparticle Delivery System

The designed fume suppression system shown in Figure 1 consisted of a powered base unit and equipment called a NanoMix canister. An ordinary (Carbon dioxide) CO₂ shielding gas was connected to the welding machine. The shielding gas host from the welding machine was connected to the inlet of the NanoMix canister and out to the regular welding gun. This was the only modification during installation for by-passing the shielding gas to the NanoMix canister. Upon operation, shielding gas passed through the canister picking up the suspended nanoparticles from the agitation of the powered base unit mechanism. As a result, the nanoparticles were mixed into the stream of CO₂ shielding gas. To be noted, the content of NanoMix is commercialized mainly as ZnO (Zinc Oxide) but could not be revealed in detail owing to the trade secret that has been licensed to a company under a set of patents filed by KMUTT. While ZnO has a comparable bandgap to TiO₂ for free-electron generation via photocatalytic reaction, ZnO is a substance providing white color in the cosmetic industry making it safe to use.

The nanoparticle contents in the canister experimented with 3 shielding gas flow rates: 10, 15, and 25 Liter per Minute (LPM). The reason for using such a high flow rate of 25 LPM was due to the requirement in the actual working conditions. Even though it was not recommended in welding practice, it was a requirement from our market-focused groups. The content of nanoparticles in the canister was set at 2, 5, 8, and 10 grams. The target was to operate the system for at least 10 hours of arc time before refilling the canister. This was the same operating duration of 1 cylinder of the CO₂ shielding gas.

The number of delivered nanoparticles was performed using the given factors by blowing the shielding gas stream for 3 minutes on the glass fiber filler brand Advantec Grade GB-140 with 0.4 μm pore size with 47 mm in diameter. The weight gain of the filler was used for the number of delivered nanoparticles.

Welding Procedures

Chemical compositions of base material and welding wire were shown in Table 1. The specimen size was 300 x 300 x 10 mm. The welding consumable was flux-cored wire grade E71T-1C with 1.2 mm in diameter. The bead on plate weld was performed using mechanized equipment to control the travel speed at 5 mm/s. A welding operation was performed inside the fume hood for fume collection using CO₂ shielding gas for 1 minute. Welding current was set at 220 Ampere with 24 V using (Direct Current Electrode Positive) DCEP polarity. The contact tip to work distance (CTOD) was fixed at 12 mm (approx.) for arc stability.

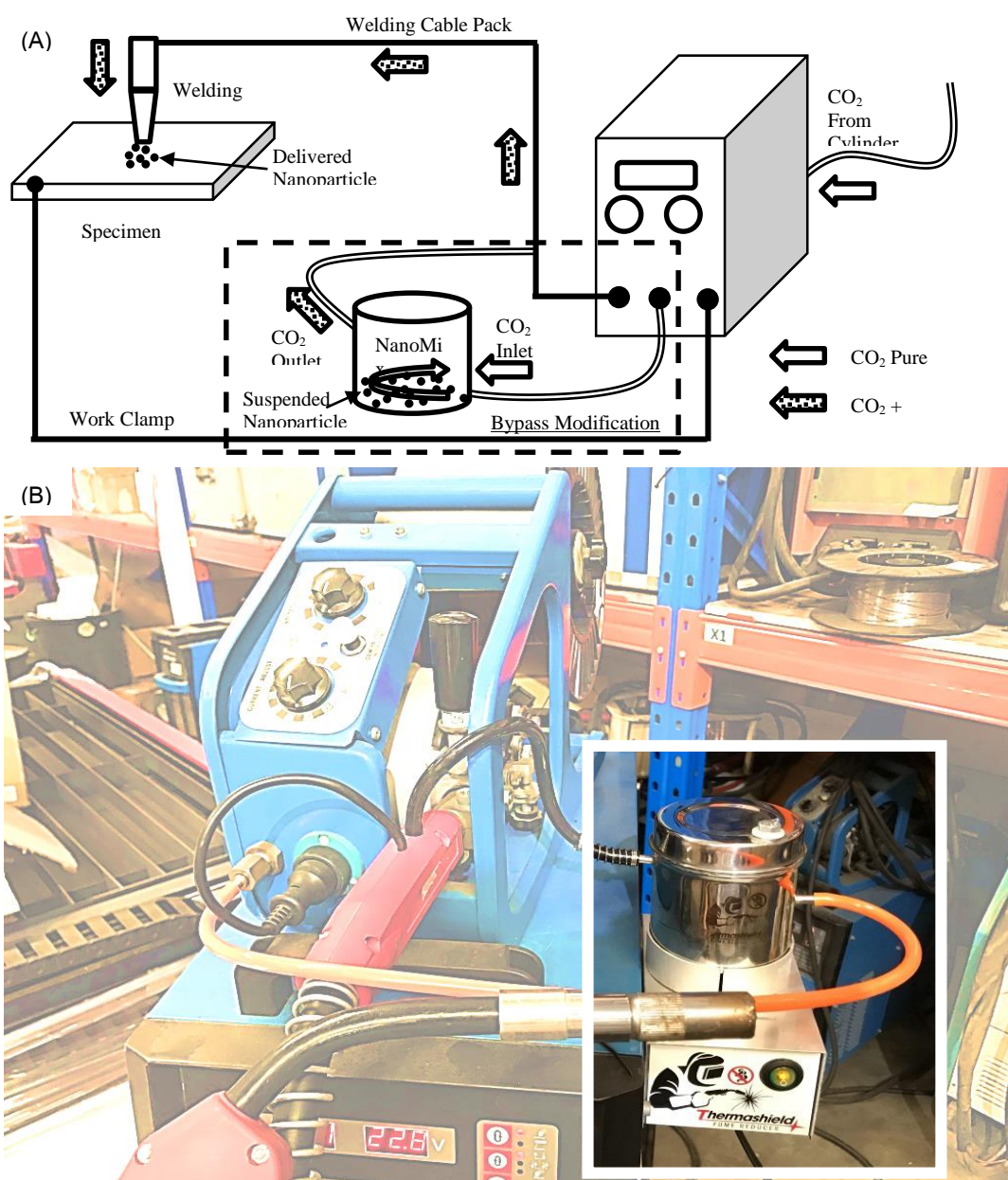


Figure 1 Schematic diagram of nanoparticle delivery system (A) and actual setup of nanoparticle fume suppression system (B).

Table 1 Nominal composition of base material and welding wire (%wt)

Materials	C	Si	Mn	P
SS400	0.142	0.279	0.720	0.022
E71T-1C	0.05	0.47	1.39	0.01

Fume Hood Verification

The fume hood was designed as a rectangular box shown as in Figure 2. Since the fume generation rate (FGR) changes with the arc voltage, the verification was performed using a solid wire grade ER70G in 1.2 mm diameter with the arc voltage of 24, 26, and 28 V. Welding fume generated were collected after the end of 1-minute welding for 5 minutes duration. The fume collection media was adapted from the roof insulation as it is made of glass fiber. Its size was about 120 mm in diameter and 75 mm in thickness. It was cut using a circular pattern for sizing so that its weight was controlled at about 12 ± 1 grams to maintain its density for the consistency of the fume collection performance. The experiments were performed with at least 3 replications for the reliability of the data. Even though the welding electrode was not ER70s-3 as stated in the AWS F1.2 standard [20], its performance could be verified relatively. Verification results were shown in Figure 3. In comparison to the standard, the collected fume contents were lower but its behavior still showed the same trend as expected by the standard. Therefore, the fume hood and fume collection procedure could be applicable for the relative comparison.

Fume Measurement

A bead on plate weld was performed using the welding parameters stated in the previous section. The arc time was set at 1 minute, then the suction system of the fume hood would be started allowing for another 5 minutes for fume collection. The weight gained from glass fiber was used for the amount of welding fume collected. The fume generation rate was measured and compared to the baseline in which none of the nanoparticles introducing to the shielding gas. In addition, the welding current levels were also investigated on the fume reduction capability limit. This would represent the robustness of the fume suppression system at the low welding current. Again, there were at least 3 replications of an experiment for reliable results.

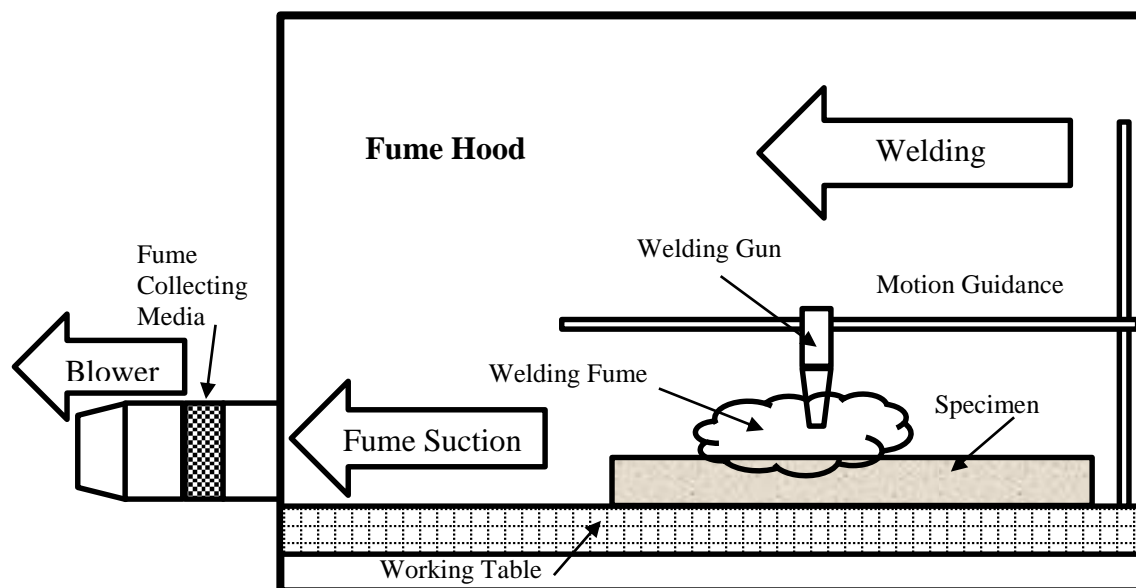


Figure 2 Schematic diagram of fume collection hood.

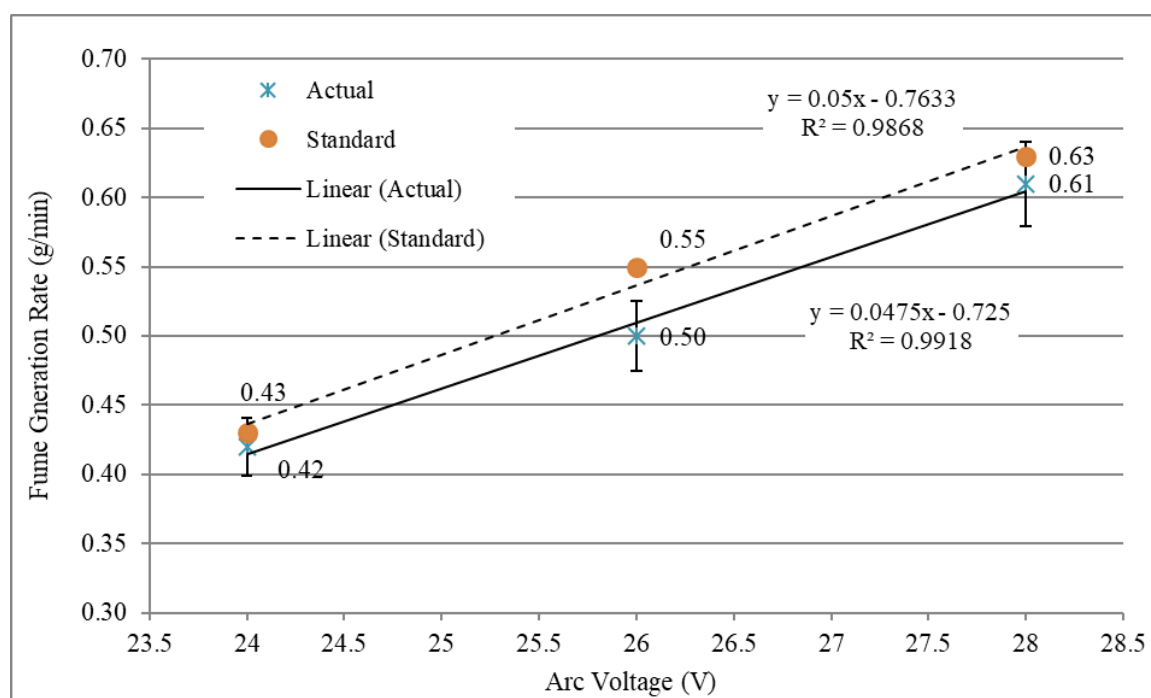


Figure 3 Fume hood verification results.

Weld Performance Tests

To determine any detrimental effect of nanoparticles, the actual weld performance test was performed. ASME BPVC.IX [21] was implemented for the welding procedure qualification test. The weldment was performed on 150 x 300 x 10 mm plates with the joint design and welding sequences as shown in Figure 4. After welding, 2 tensile tests and 4 side bend tests were performed. The mechanical tests were performed by the ISO/IEC17025:2017 accredited facility for the validity of the test results.

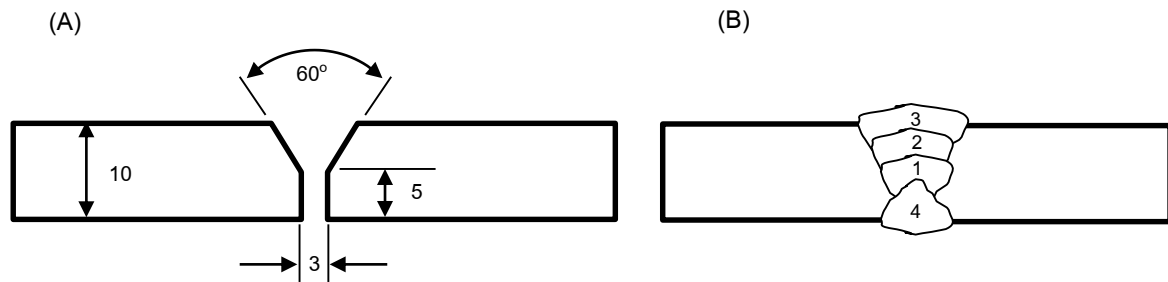


Figure 4 Joint design; unit in mm (A) and actual welding sequences (B) for performance test weld.

Microstructure and Trace Element Evaluation

The residues of ZnO nanoparticles might enter the weld pool during welding either by melting or deposition. This could alter the weld metal microstructures and cause a detrimental effect on the weldment. Weld metal microstructure must be evaluated. The specimens were prepared from the blank remaining from the weld performance tests. An ordinary microstructural preparation was performed by grinding using SiC papers in steps from #220, #400, #800, and #1200, then polishing using 1 μm diamond suspension, followed by etching 2% Nital solution. Scanning Electron Microscope (SEM) was implemented to observe the weld metal microstructure. Energy Dispersive Spectrometry (EDS) hook-up with the SEM was used to determine the chemical composition of the weld metal microstructure for any possible trace of Zn that could deposit on the specimens.

Results and Discussion

Nanoparticle Delivery

The nanoparticle delivery system performance versus nanoparticle content in the canister as shown in Figure 5 for each CO_2 shielding gas flow rate, the gas flow rates had a stronger effect on the delivery rate, especially at high content of nanoparticles. It could deliver up to about 28.98 mg/min (raw data) at 25 LPM of gas flow rate and 10 grams of the contents. On the other hand, from the calculated relationship equation shown in Figure 5, it could deliver about 32.98 mg/min at the same factors. Even though, as the delivery rate decreased with the decrease of contents, the nanoparticle contents in the canister could still be sufficient for welding operation up to 10 hours of the arc time conforming to the usage of 1 cylinder of CO_2 shielding gas. The canister has been designed as refillable, so it could be replaced at the same time as changing the shielding gas cylinder.

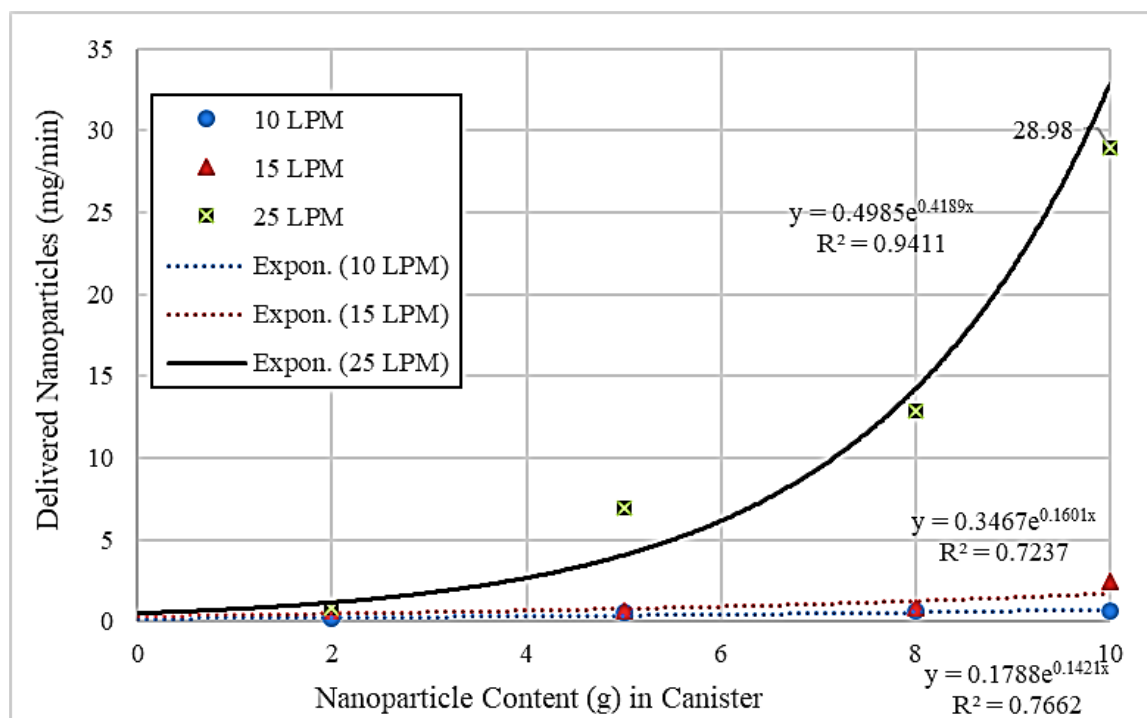


Figure 5 Delivered nanoparticles with shielding gas flow rates and nanoparticle contents in the canister.

Even though, the delivered nanoparticles decreased as the contents in the canister decreased, its delivered content was still effective (as little as two grams) for the fume suppression process according to the results in the next section. For other shielding gas flow rates, the number of delivered nanoparticles was drastically decreased but the delivered contents were still effective to reduce the fume generation to a lower extent. As stated in the experimental procedure section, this system was designed to serve the focused groups that required high shielding gas flow rate. Therefore, the internal parts of the canister were designed accordingly, resulting in less delivered nanoparticle contents at the lower shielding gas flow rates.

Effect of Gas Flow Rate on Fume Reduction

For comparison, the above-given welding parameters were implemented for both without nanoparticles as the baseline and with nanoparticles. The results were shown in Figure 6(A), (B), and (C) for the front side, through-thickness, and the rear side of collection media consecutively compared to the Figure 6 (D), (E), and (F) which nanoparticles were introduced at the flow rate of 25 LPM. There was significantly more fume collected at the front side of the baseline welding without nanoparticles. Some fume could leak through the sidewall of the fume collecting fixture to the rear side of the collection media as can be seen in Figure 6 (F). Even with leak fume, the fume collected in the case of nanoparticles used was still lower showing their ability for fume reduction.



Figure 6 Glass fiber after fume collection for regular shielding gas: front (A), side (B), and rear (C), and for nanoparticles mixed at 25 LPM and 10 grams in the canister: front (D), side (E), and rear (F).

To determine the effect of both shielding gas flow rate and the nanoparticle contents in the canister, an Analysis of Variance (ANOVA) was performed. The results shown in Table 2 suggested that both factors had significant effects on the fume reduction rate as the P-value were 8.09×10^{-11} and 3.92×10^{-14} for nanoparticle contents and the shielding gas flow rates consecutively. In addition, the interaction of both factors also had a significant effect at the P-value of 1.07×10^{-5} .

Table 2 ANOVA of Nanoparticle contents in the canister and Shielding gas flow rates

<i>Source of Variation</i>	<i>SS</i>	<i>df</i>	<i>MS</i>	<i>F</i>	<i>P-value</i>
Nanoparticle Contents	0.048951	3	0.016317	53.97794	8.09×10^{-11}
Shielding gas flow rates	0.087782	2	0.043891	145.1961	3.92×10^{-14}
Interaction	0.018841	6	0.00314	10.38829	1.07×10^{-5}
Within	0.007255	24	0.000302		
Total	0.162829	35			

To discuss further, the shielding gas flow rates were individually determined and the results were shown in Figure 7. The Fume Generation Rate (FGR) was higher at high shielding gas flow rates. Following the addition of nanoparticles, the FGR at the shielding gas flow rate of 25 LPM were 0.61, 0.58, 0.58, and 0.58 g/min for 2, 5, 8, and 10 grams of contents in the canister, respectively. In contrast, the baseline was at 0.84 g/min showing the effectiveness on the fume reduction. For each nanoparticle content in the canister, the FGR was also higher for high shielding gas flow rates. This might suggest that the nanoparticles themselves also had a contribution to fume generation as more nanoparticles were delivered. Another reason would be the turbulence caused by the high gas flow rate picking up oxygen from the surrounding resulting in more fume generation. However, the effectiveness of nanoparticles in fume reduction was still predominant.

As can be seen in Figure 7 (B), the %FGR reduction was higher for high shielding gas flow rates as a result of more delivered nanoparticles compared to the lower flow rates. Up to 30.28% of fume reduction at 10 grams and 25 LPM could be achieved and decreased to 27.09% as the contents decreased to 2 grams. This was drastically higher compared to the 10 LPM flow rate that could reduce the fume generation rate to only 19.89% at 10 grams contents and decreased to 11.05% after remaining to 2 grams of contents. This suggested that both shielding gas flow rates and contents in the canister affected the %FGR conforming to the ANOVA results. Figure 8 showed the relationship between %FGR reduction and nanoparticle delivery rate. The rate around 0.5 mg/min and above would result in at least 20%FGR reduction. Nevertheless, a higher delivery rate would not provide a significantly better %FGR reduction while too low delivery rate resulted in a very low %FGR reduction. This suggested that too-high delivered nanoparticles would not be beneficial as their ability in fume reduction might not be able to overcome the fume formation from their burning effect. As a result, the content in the canister would not be too much than 10 grams and the internal parts of the canister would be designed for the 25 LPM shielding gas to prevent excessive delivered nanoparticles.

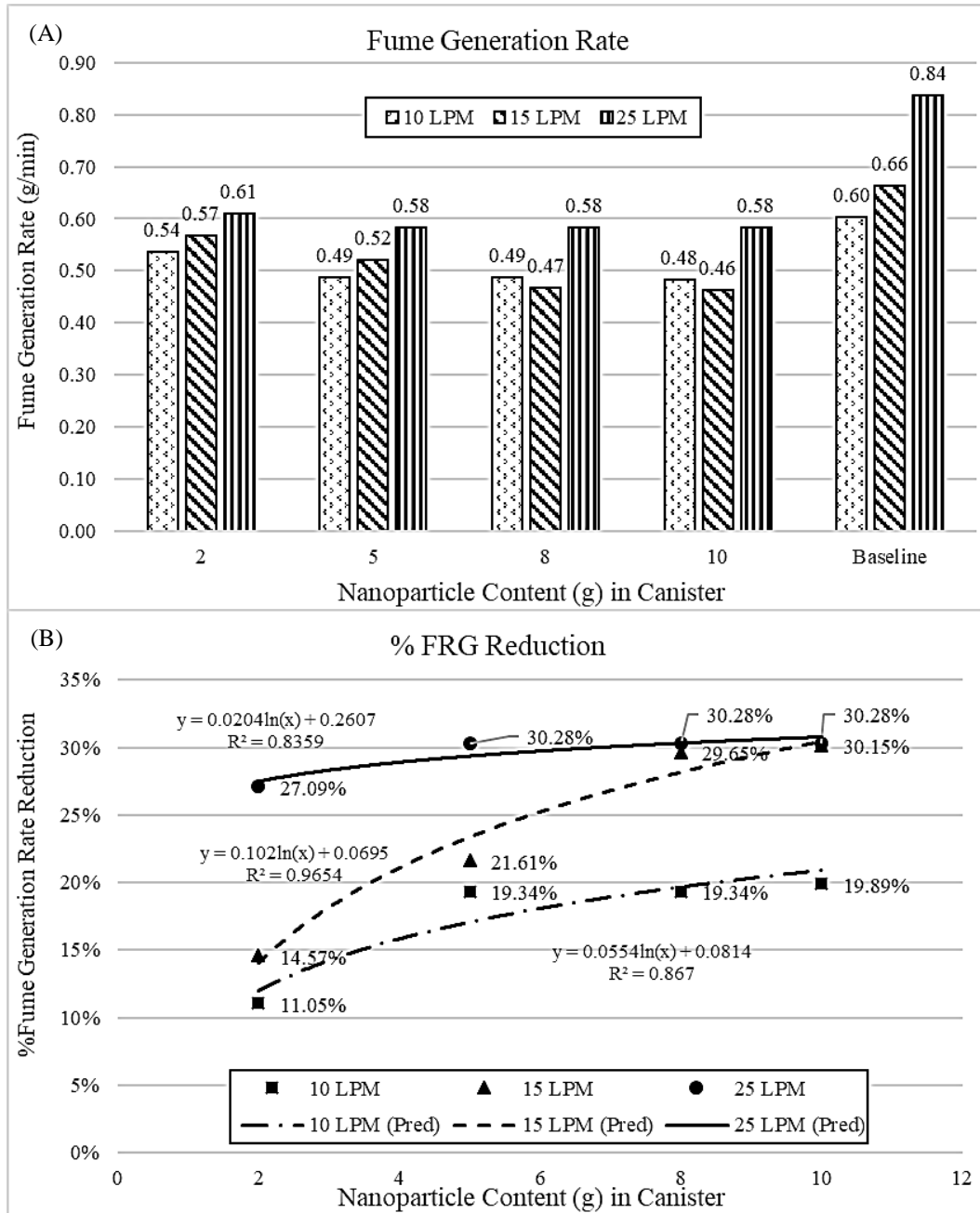


Figure 7 Fume generation rate (A) and %FGR reduction (B) after adding nanoparticles to the shielding gas stream.

According to the results above, the effectiveness of the fume suppression rate was affected by the shielding gas flow rates and the contents of nanoparticles which in turn was the number of delivered nanoparticles. Any combinations that could deliver a sufficient amount of nanoparticles could be eligible. In this case, the shielding gas flow rate of 25 LPM was preferred because of the actual working conditions of our target groups that used this flow rate or higher, even though, it was not recommended due to the turbulence possibly generated. On the other hand, the lower shielding gas flow rates resulted

in fewer nanoparticles delivered causing less fume reduction. To overcome this limitation, a new internal design of the canister must be performed in the future design.

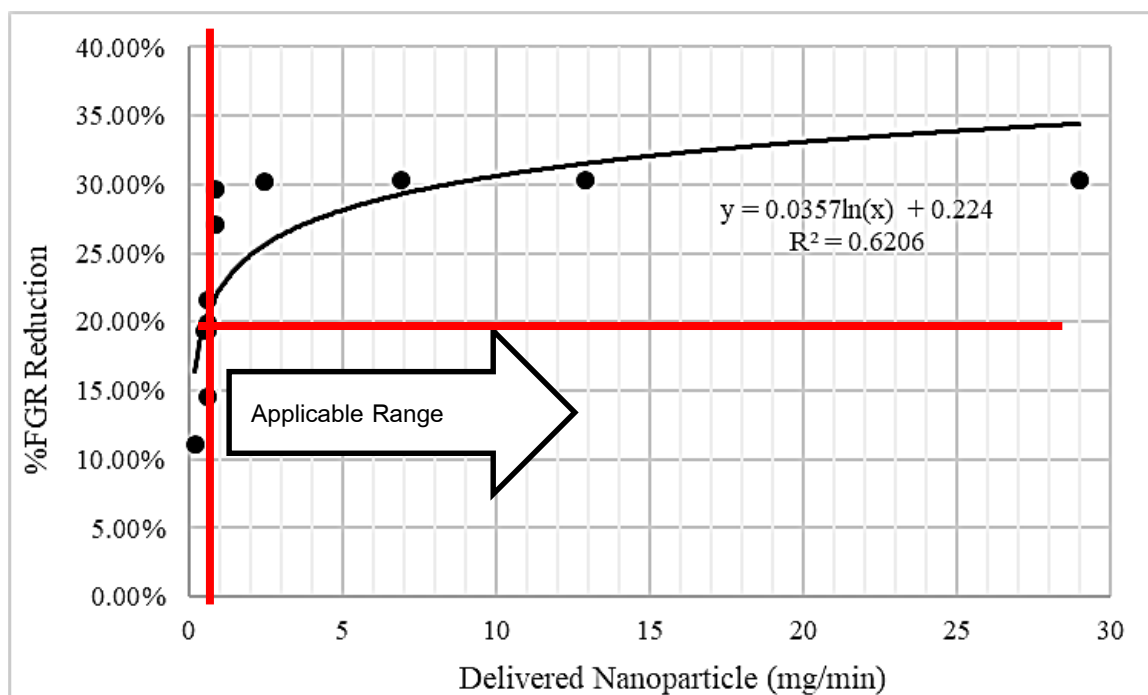


Figure 8 Effect of delivered nanoparticle rate and %FGR reduction.

Effect of Welding Current and Proposed Mechanism

FGR measured in the previous section were performed at the welding current of 220 A. To determine the robustness of the system, the variation of welding current levels should be evaluated. As shown in Figure 9, the welding current was decreased to 200, 150, and 120 A while other parameters remained the same. Baseline FGR was decreased due to lower weld heat input from 0.84 g/min to 0.62 g/min and 0.25 g/min (220, 200, and 120 A). Nanoparticles were still effective to reduce the FGR from 0.62 g/min to 0.44 g/min (29.95%) at 200 A welding current. The effectiveness decreased as the welding current decreased which resulted in %FGR at 21.33% at a welding current of 120 A. This was due to the lower current that caused lower light or radiation necessary for the photocatalytic reaction of nanoparticles. Nevertheless, the %FGR was all above 20% even reaching the lower limit welding current of the FCAW that was capable of producing the sound weld.

The proposed fume reduction mechanism was referred as the fume formation mechanism proposed by Gonser and Hogan [22] indicating that the welding fumes form in various types of oxides. Metal droplets or vapor could be oxidized as they migrate out of the pocket of shielding gas reacting with oxygen in the atmosphere. If one could prevent this formation by reducing the oxidation state of metals before contact with the oxygen, the fume formation would be suppressed.

In this proposed system, the nanoparticles mixed into the shielding gas stream would undergo the photocatalytic reaction [23] with the light or radiation provided by the arc column during welding resulting in free-electron generation. These electrons would then neutralize the oxidized metals that escaped from the arc column making them be at the zero oxidation state before reacting with the oxygen suppressing the ability of metal ions to react with the oxygen and form the metal oxides which in turn the fume generation, Therefore, only the metal vapor remained and condensed as particles which either escaped from the weld or dropped on the specimen.

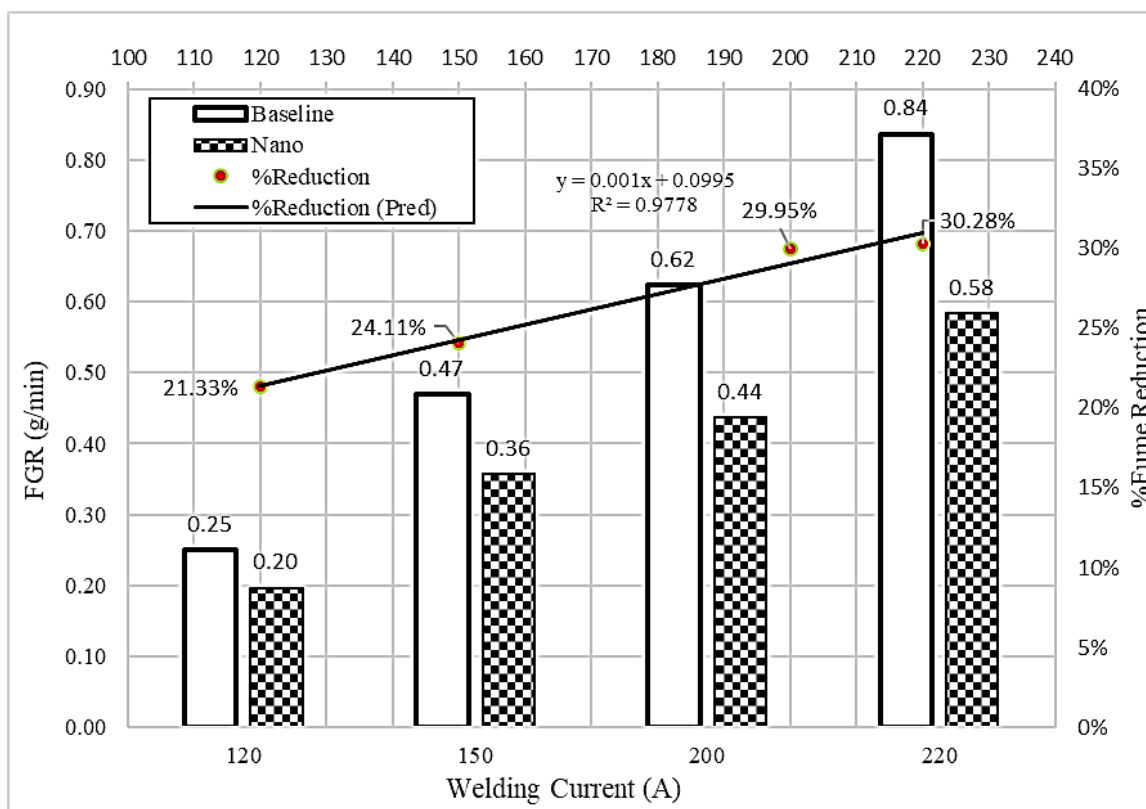


Figure 9 Effectiveness of nanoparticles on FGR at various welding currents.

Table 3 Calculation of metal remains from fume suppression process (without oxide formation)

Atomic Weight				
Mn	54.94			
Fe	55.84			
O	16.00			
Types of Fume	Molecular Weight	Weight Remain		%Reduction
Fe ₃ O ₄	231.52	3Fe	167.52	27.64%
MnFe ₂ O ₄	230.62	Mn+2Fe	166.62	27.75%
FeMn ₂ O ₄	229.72	Fe+2Mn	165.72	27.86%
x-MnO ₂	86.94	Mn	54.94	36.81%
x-Fe ₂ O ₃	159.68	2Fe	111.68	30.06%

Example calculations were provided in Table 3. For welding fume as Fe_3O_4 , its molecular weight was 231.52 grams. But if there were only 3 atoms of Fe (without 4 oxygen atoms) the total weight would be 167.52 grams which was a 27.64% reduction. The same would apply to MnFe_2O_4 with molecular weight of 230.62 grams, while the only metals (1 Mn and 2 Fe) would be 166.62 grams (27.75% reduction). These calculations conformed to the experimental results that the %FGR reduction was about 20–30% depending on the delivered nanoparticles and welding current levels. These showed the evidence that the “prior-reduction” process by photocatalytic reaction of nanoparticles with the radiation from the arc column would be effective for fume reduction.

Weld Performance

Another aspect that needs to be considered is the performance of the weldment as it could be affected by the nanoparticles mixed into the weld metal. Welding Procedure Specification (WPS) and Procedure Qualification Record (PQR) were implemented according to the ASME BPVC.IX [21] for 2 tensile specimens across the weldment and 4 side bend tests. The results are shown in Table 4. All tensile specimens failed at the base material indicating that there was no detrimental effect of nanoparticles as the weld metal was stronger than the base material. The side bend specimens showed an opened indication on only 1 specimen with a size of 0.66 mm. This might be due to the skill of the welder causing the formation of either incomplete fusion or slag inclusion. However, since the opened indication size was below the 3 mm limit indicated by the ASME standard, the WPS was acceptable based on the PQR results confirming that the nanoparticles did not have any detrimental effect on the weldment.

Table 4 Results of weld performance tests

Types of Test	Results/Indication	Remark
Tensile 01	461.46 MPa	Base Material
Tensile 02	466.72 MPa	Base Material
Side Bend 01	Not Found	N/A
Side Bend 02	0.66 mm	< 3 mm
Side Bend 03	Not Found	N/A
Side Bend 04	Not Found	N/A

Microstructure and Trace Elements

Another perspective problem was related to the weldability caused by the mixing or melting of nanoparticles, which is Zn in this case, into the weld pool resulting in detrimental changes in the weld metal. Microstructures of weld metal were shown in Figure 10 which presented the microstructures consisting the columnar solidification as usual for welding. There was no evidence of any small crack. Both the top layer and back weld were not significantly different. The chemical composition of weld metal was also analyzed by as EDS shown in Figure 11. Weld metal compositions were as usual for

the plain carbon steel having Fe as balance with Mn and Si as trace elements in bulk. For the point scan technique at the suspected feature, in Figure 11 (B), the results showed Ti and F were the ordinary ingredients of flux commercially. On the other hand, if the Zn showed in the weld metal composition, it represents the risk of weld metal cracking and affects the weldability.

From the results, there was no evidence of Zn as the trace of nanoparticles found in the weld metal by composition analysis. Since the welding process used in this study was FCAW, the flux that came with the welding wire could help to clean the weld pool. In this case, any remain of Zn could be captured by the flux and then solidified mixed with the slag covered on the weld metal.

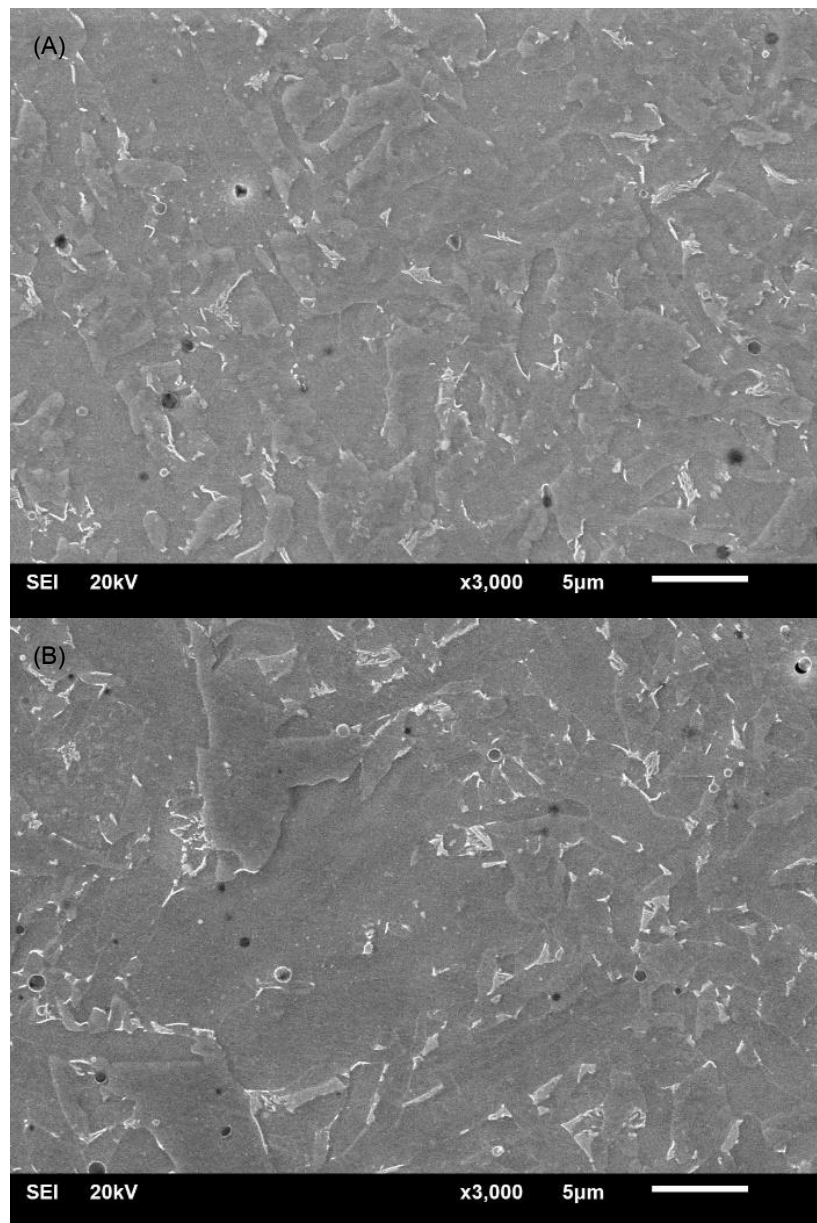


Figure 10 Microstructure of the weld metal: Top layer (A) and Back weld (B).

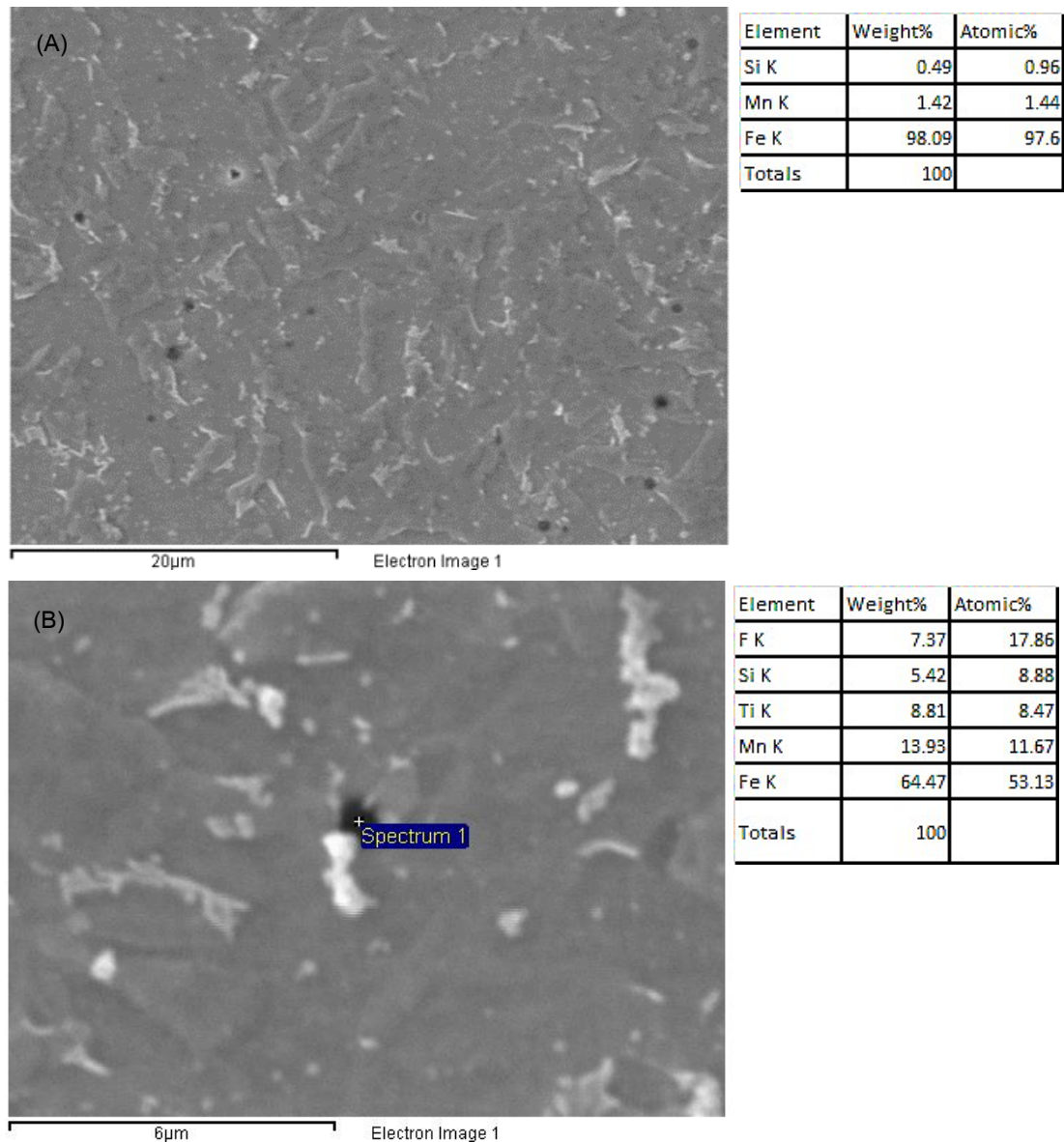


Figure 11 SEM/EDS composition analysis for nanoparticle residue: Area scan (A) and Point scan (B).

Conclusions

A developed fume reduction system for FCAW by mixing nanoparticles into the shielding gas stream was evaluated both for fume reduction performance and its prospective detrimental effects. The system could be implemented in the actual welding as the add-on equipment without the necessity for adjusting the exiting parameters. The results from implementing the system could be summarized as the following;

1. Nanoparticles could be delivered to the tip of the welding gun with the amount depending on the shielding gas flow rates and the nanoparticle contents in the canister.
2. Delivered nanoparticles could be effective on %FRG reduction.

3. The contents of nanoparticles in the canister had less effect compared to the shielding gas flow rates. However, too low contents resulted in low %FGR.
4. The fume reduction system was robust and could be operated at low welding current up to 120 A with %FGR reduction beyond 20%.
5. The proposed mechanism for fume reduction was a “prior-reduction” reaction was conformed to the experimental results. The FGR was comparable to the reduction of molecular weight of Fe_3O_4 .
6. Weld performance could not be compromised by the mix of nanoparticles as the WPS and PQR were conformed to the ASME BPVC.IX standard.
7. From the microstructure and SEM/EDS of weld metal, there was no trace of Zn from nanoparticles presented in the weld metal.

Acknowledgements

This research was granted under the Research Gap Fund 2019 program in co-funding between the National Science and Technology Development Agency (NSTDA), Ministry of Higher Education, Science, Research and Innovation (MHESI), and Thermal Mechanic Co. Ltd.

References

1. Antonini, J. M. (2003). Health effects of welding. *Critical Review in Toxicology*, 33, 61-103.
2. Roach, L. L. (2018). The Relationship of welding fume exposure, smoking, and pulmonary function in welders. *Workplace Health & Safety*, 66, 34-40.
3. MacLeod, J. S., Harris, M. A., Tjepkema, M., Peters, P. A., & Demers, P. A. (2017). Cancer risks among welders and occasional welders in a national population-based cohort study: Canadian census health and environmental cohort. *Safety and Health at Work*, 8, 258-266.
4. Changa, Y. J., Sproesserb, G., Neugebauer, S., Wolf, K., Scheumann, R., Pittner, A., Rethmeier, M., & Finkbeiner, M. (2015). Environmental and social life cycle assessment of welding technologies. *Procedia CIRP*, 26, 293-298.
5. Jenkins, N. T., & Eagar, T. W. (2005). Chemical analysis of welding fume particles. *Welding Journal*, 84, 87s-93s,
6. Sowards, J. W., Ramirez, A. J., Lippold, J. C., & Dickinson, D. W. (2008). Characterization procedure for the analysis of arc welding fume. *Welding Journal*, 87, 76s-83s.
7. Sowards, J. W., Lippold, J. C., Dickinson, D. W., & Lippold, J. C. (2008). Characterization of welding fume from SMAW electrodes-Part I. *Welding Journal*, 87, 106s-112s.
8. Cena, L. G., Chen, B. T., & Keane, M. J. (2016). Evolution of Welding fume aerosols with time and distance from the source. *Welding Journal*, 95, 280s-285s.
9. Jeong, J. Y., Park, J. S., & Kim, P. G. (2016). Characterization of total and size-fractionated manganese exposure by work area in shipbuilding yard. *Safety and Health at Work*, 7, 150-155.

10. Meeker, J. D., Susi, P., & Flynn, M. R. (2007). Manganese and welding fume exposure and control in construction. *Journal of Occupational and Environmental Hygiene*, 4, 943-951.
11. Gonser, M. J., Lippold, J. C., Dickinson, D. W., Sowards, J. W., & Ramirez, A. J. (2010). Characterization of welding fume generated by high-Mn consumables. *Welding Journal*, 89, 26s-33s.
12. Redding, C. J. (2002). Fume model for gas metal arc welding. *Welding Journal*, 81, 95s-103s.
13. Dennis, J. H., Hewitt, P. J., Redding, C. A. J., & Workman, A. D. (2001). A model for prediction of fume formation rate in gas metal arc welding (GMAW), globular and spray modes, DC electrode positive. *The Annals of Occupational Hygiene*, 45, p. 105-113.
14. Zaidi, S., Sathawara, N., Kumar, S., Gandhi, S., Parmar, C., & Saiyed, H. (2004). Development of indigenous local exhaust ventilation system: reduction of welders exposure to welding fumes. *Journal of Occupational Health*, 46, 323-328.
15. Turker, N., Bilirgen, H., Viecco, G. A., & Caram, H. S. (2005). Development of a lightweight fume hood for handheld welding guns. *Welding Journal*, 84, 31s-36s.
16. Castner, H. (1995). Gas metal arc welding using pulsed fume generation current. *Welding Journal*, 74, 59s-68s.
17. Meneses, V. A., Gomes, J. F. P., & Scotti, A. (2014). The effect of metal transfer stability (spattering) on fume generation, morphology and composition in short-circuit MAG welding. *Journal of Materials Processing Technology*, 214, 1388-1397.
18. Sowards, J. W., Liang, D., Alexandrov, B. T., Frankel, G. S., & Lippold, J. C. (2011). A new chromium-free welding consumable for joining austenitic stainless steels. *Welding Journal*, 90, 63s-76s.
19. Mohan, S., Sivapirakasam, S. P., Kumar, M. C. S., & Surianarayanan, M. (2015). Welding fume reduction by coating of nano-TiO₂ on electrodes. *Journal of Materials Processing Technology*, 219, 237-247.
20. AWS. (1999). F1.2: *Laboratory Method for measuring fume generation rates and total fume emission of welding and allied processes*. Miami, Florida, USA.
21. ASME. (2019). BPVC. IX: *Qualification Standard for welding, brazing, and fusing procedures; welders; brazers; and welding, brazing, fusing operators*. New York, USA
22. Gonser, M., & Hogan, T. *Arc welding health effects, fume formation mechanisms, and characterization methods*. Retrieved August 21, 2020, from <https://www.intechopen.com/books/arc-welding/arc-welding-health-effects-fume-formation-mechanisms-and-characterization-methods>
23. Beydoun, D., Amal, R., Low, G., & McEvoy, S. (1999). Role of Nanoparticles in Photocatalysis. *Journal of Nanoparticle Research*, 1, 439-458.